HHS Public Access

Author manuscript

Headache. Author manuscript; available in PMC 2019 January 01.

Published in final edited form as:

Headache. 2018 January ; 58(1): 88–101. doi:10.1111/head.13188.

Quantitative analysis of mouse dural afferent neurons expressing TRPM8, VGLUT3 and NF200

Lynn Ren, BS[1], **Michelle Jaehee Chang, BS**[1], **Zhiyu Zhang, BS**[1], **Ajay Dhaka, PhD**[2], **Zhaohua Guo, PhD**[1], and **Yu-Qing Cao, PhD**[1]

[1]Washington University Pain Center and Department of Anesthesiology, Washington University School of Medicine, St. Louis, MO 63110, USA

[2]Department of Biological Structure, Neurobiology and Behavior Graduate Program, University of Washington, Seattle, WA 98195, USA

Abstract

Objective—To quantify the abundance of dural afferent neurons expressing transient receptor potential channel melastatin 8 (TRPM8), vesicular glutamate transporter 3 (VGLUT3) and neurofilament 200 (NF200) in adult mice.

Background—With the increasing use of mice as a model system to study headache mechanisms, it is important to understand the composition of dural afferent neurons in mice. In a previous study, we have measured the abundance of mouse dural afferent neurons that express neuropeptide calcitonin gene-related peptide as well as two transient receptor potential channels TRPV1 and TRPA1, respectively. Here, we conducted quantitative analysis of three other dural afferent subpopulations in adult mice.

Methods—We used the fluorescent tracer Fluoro-Gold to retrogradely label dural afferent neurons in adult mice expressing enhanced green fluorescent protein in discrete subpopulations of trigeminal ganglion (TG) neurons. Mechanoreceptors with myelinated fibers were identified by NF200 immunoreactivity. We also conducted Ca^{2+}-imaging experiments to test the overlap between TRPM8 and VGLUT3 expression in mouse primary afferent neurons (PANs).

Results—The abundance of TRPM8-expressing neurons in dural afferent neurons was significantly lower than that in total TG neurons. The percentages of dural afferent neurons expressing VGLUT3 and NF200 were comparable to those of total TG neurons, respectively. TRPM8 agonist menthol evoked Ca^{2+} influx in less than 7% VGLUT3-expressing PANs in adult mice.

Conclusions—TG neurons expressing TRPM8, VGLUT3 and NF200 all innervate adult mouse dura. TRPM8 and VGLUT3 are expressed in distinct subpopulations of PANs in adult mice. These results provide an anatomical basis to investigate headache mechanisms in mouse models.

Correspondence to: Zhaohua Guo; Yu-Qing Cao.

Conflict of Interest: None

Keywords

migraine; headache; TRPM8; VGlut3; NF200; dural afferent neurons

Background and Objective

Recent years have seen a rapid increase in the use of mouse as a model system to study the pathophysiology of headache. It is well established that the activation and sensitization of the primary afferent neurons (PANs) innervating the dura and cerebral blood vessels play a crucial role in the onset and maintenance of a headache episode [1-3]. Quantitative assessment of the dural afferent neuron subpopulations in mice provides an anatomical basis for functional studies to gain insights into headache mechanisms using mouse models. In a previous study, we have measured the abundance of dural afferent neurons that express neuropeptide calcitonin gene-related peptide (CGRP), transient receptor potential (TRP) channel subfamily V member 1 (TRPV1) and subfamily A member 1 (TRPA1), respectively [4]. However, using fluorescent retrograde tracer DiI (1,1′-dioctadecyl-3,3,3′,3′-tetramethylindocarbocyanine perchlorate), we were not able to label the cell body of dural afferent neurons expressing TRP channel melastatin 8 (TRPM8) in mouse trigeminal ganglion (TG), despite the fact that TRPM8-expressing fibers are known to be present on mouse dura [5, 6] and dural TRPM8 channels have been shown to regulate headache-related behaviors in rodent models [6-8]. This presents a technical hurdle for further investigation of the neurochemical and physiological properties of TRPM8-expressing dural afferent neurons. We speculated that sparse meningeal innervation and lack of extensive axonal branches might limit the likelihood and/or the amount of tracer taken up by individual TRPM8-expressing dural afferent neurons [6].

The first objective of this study is to test whether another retrograde tracer Fluoro-Gold (FG) is more efficient than DiI in labeling dural afferent neurons in mice. And if so, whether we can use FG to quantify the abundance of TRPM8-expressing dural afferent neurons in heterozygous mice that express farnesylated enhanced green fluorescent protein (EGFPf) at one TRPM8 locus ($TRPM8^{EGFPf/+}$). Secondly, many dural afferent neurons are mechanosensitive [9]. Sensitization of these neurons contributes to the intracranial mechanical hypersensitivity during headache [3]. Thus, our second objective is to quantify the abundance of mechanoreceptors with myelinated and unmyelinated fibers in dural afferent neurons, using the expression of neurofilament 200 (NF200) and the expression of vesicular glutamate transporter 3 (VGLUT3) as respective markers. Lastly, in light of a recent report that TRPM8 channel is expressed in a subpopulation of small diameter dorsal root ganglion (DRG) neurons that express VGLUT3 in adult mice and/or during development [10], we investigated whether TRPM8 agonist menthol activates PANs that persistently express VGLUT3 in adult mice, using transgenic mice that express EGFP under the control of *Vglut3* regulatory sequences ($VGLUT3^{EGFP}$).

Methods

Mice

All procedures were carried out in strict accordance with the recommendations in the Guide for the Care and Use of Laboratory Animals of the National Institutes of Health and the guidelines of the Animal Study Committee at Washington University in St. Louis. Mice were housed on a 12-hour light-dark cycle with food and water available *ad libitum* at the animal facility of Washington University in St. Louis. Eight-twelve weeks old adult mice (14 male and 16 female) were used in this study. Data from male and female mice were combined for statistical analysis as there was no sex difference in the mean value of any of the parameters we measured. TRPM8$^{EGFPf/+}$ mice expressing EGFPf at one TRPM8 locus [11] were maintained on CD-1 background. The VGLUT3^{EGFP} transgenic mice that express EGFP under the control of *Vglut3* regulatory sequences [12] were maintained on C57BL6 background. The genotype was determined by PCR of tail DNA as described previously [11, 12]. Wild-type mice on C57BL6 background were used to study NF200 expression and the labeling efficiency of FG and DiI in dural afferent neurons.

Retrograde labeling of TG neurons innervating mouse dura

On the surgery day, mice were anesthetized with 3-4% isoflurane in an induction chamber until losing the righting reflex and were mounted on a Stoelting stereotaxic apparatus. Anesthesia was maintained by 1.5-2% isoflurane through a nose cone. Body temperature was maintained by placing mice on a 37°C circulating water warming pad. A small amount of eye drops was placed in the eyes to prevent the corneas from drying. Lidocaine hydrochloride jelly (2%) was applied on the skin for 5 minutes (min) before a longitudinal skin incision was made to expose the cranium. Lidocaine was then applied on the exposed tissue for 5 minutes before the muscle and periosteal sheath were removed in the area overlying the superior sagittal sinus (SSS) between bregma and lambda. A craniectomy (~2.5 mm diameter) was made with a surgical blade within this area, leaving the underlying dura exposed but intact. Lidocaine was repetitively applied on the skull during the craniectomy to prevent the activation and/or sensitization of the PANs. To prevent the spreading of the tracer to other peripheral sites, a sterile polypropylene ring was sealed to the skull surrounding the exposed dura by a mixture of dental cement powder (Stoelting 51459) and superglue adhesive. The viscosity of dental cement/superglue mix kept it from spreading to the exposed dura. After waiting 5-10 min for the mix to solidify, we applied 20 μl of FG (2% in 0.9% saline, Fluorochrome) onto the exposed dura. In some mice, we co-applied DiI (2%, Invitrogen) and FG (2%) to the dura in 20 μl saline solution with 10% DMSO. Subsequently, a sterile polypropylene cap was secured over the ring with the dental cement/ superglue mix to cover the exposed dura. The skin incision was closed with Vetbond tissue adhesive. After recovery from anesthesia, mice were housed individually in the animal facility for 14 days to allow for the transport of the tracers to the dural afferent somata in TG.

Tissue Preparation and Immunohistochemistry (IHC)

Two weeks after application of the tracers to the dura, mice were euthanized by barbiturate overdose (200 mg/kg, i.p.) and were transcardially perfused with warm 0.1 M phosphate-

buffered saline (PBS, pH 7.4) followed by cold 4% formaldehyde in 0.1 M phosphate buffer (PB, pH 7.4) for fixation. TG tissues were removed, post-fixed for 2 hours, and then protected overnight in 30% sucrose in 0.1 M PB. The ganglia were embedded in optimal cutting temperature compound (OCT) and sectioned at 20 μm using a cryostat. Sections were mounted on Superfrost Plus glass slides and stored at -20 °C. One in every three sections (cut approximately every 60 μm) was processed for each IHC experiment.

For IHC, TG sections were dried at room temperature (RT), washed three times in 0.01 M PBS and incubated in blocking buffer (10% normal goat serum [NGS], 0.3% Triton X-100, 0.01M Tris and 0.01 M PBS, pH 7.4) for 1 hour at RT. This was followed by overnight incubation of the sections in the primary antibody diluted in blocking buffer at 4°C in a humidity chamber. On the next day, sections were washed 6 times (5 min per wash) in wash buffer (1% NGS, 0.3% Triton X-100, 0.01 M Tris and 0.01 M PBS, pH 7.4) and incubated in blocking buffer for 1 hour at RT. After 1 hour incubation of the sections with the secondary antibody in blocking buffer at RT, we washed the sections 6 times (5 min per wash) in wash buffer and rinsed them 3 times in 0.01 M PBS. Finally, sections were cover-slipped using Fluoromount-G Mounting Medium (Electron Microscopy Sciences), sealed with nail topcoat and stored at 4°C for image acquisition.

The primary antibodies used were rabbit anti-EGFP (Invitrogen) at 1:1000 dilution and mouse anti-NF200 (Sigma) at 1:1000 dilution. The Alexa Fluor 568-conjugated goat anti-rabbit secondary antibody and Alexa Fluor 594-conjugated goat anti-mouse secondary antibody (both from Invitrogen) were used at 1:1000 dilution.

Image Acquisition and Analysis

Images of the TG sections were captured through a 20× objective on a Nikon TE2000S inverted epifluorescence microscope equipped with a CoolSnapHQ^2 camera (Photometrics). Cross-sectional somatic area was measured using SimplePCI software (Hamamatsu). Representative images were contrast and brightness adjusted using the same parameter within individual experiments. No other manipulations were made to the images.

Primary culture of mouse TG and DRG neurons and Ca^{2+} Imaging

TG and lumbar DRG (L3-L6) tissues were collected from 5-6 week old *TRPM8*$^{EGFPf/+}$ and VGLUT3^{EGFP} mice of either sex and were treated with 2.5 mg/ml collagenase IV followed by 2.5 mg/ml trypsin (all at 37°C, 15 min each). Cells were dissociated by triturating with fire-polished glass pipettes, seeded on Matrigel-coated coverslips and were maintained in MEM-based culture medium containing 5% fetal bovine serum, 25 ng/ml nerve growth factor and 10 ng/ml glial cell line-derived neurotrophic factor. Ca^{2+} imaging was performed in neurons 24-48 hours after plating.

On the day of imaging experiments, coverslips containing cultured neurons were incubated with HBSS/HEPES solution containing 2.5 μM fura-2 AM and 0.1% Pluronic F-127 (all from Molecular Probe) at 37°C for 30 min to load the ratiometric Ca^{2+} indicator. De-esterification of the dye was carried out by washing the coverslips 3 times with HBSS/Hepes solution and incubating the coverslips in HBSS/Hepes solution in the dark for an additional 30 min at 37°C. Neurons were used for Ca^{2+} imaging experiments within 3 hours.

Coverslips with fura-2 loaded neurons were placed in a flow chamber mounted on a Nikon TE2000S inverted epifluorescent microscope and were perfused with RT Tyrode solution (1 ml/min) containing (in mM): 130 NaCl, 2 KCl, 2 $CaCl_2$, 2 $MgCl_2$, 25 Hepes, 30 glucose, pH 7.3 with NaOH, and 310 mosmol/kgH_2O. Fura-2 was alternately excited by 340 and 380 nm light (Sutter Lambda LS) and the emission was detected at 510 ± 20 nm by a UV-transmitting 20× objective (N.A. 0.75) and a CoolSnapHQ2 camera (Photometrics). The frame capture period was 50 milliseconds at 1.5 seconds interval. SimplePCI software (Hamamatsu) was used for controlling and synchronizing the devices as well as image acquisition and analysis. EGFP fluorescence was excited at 470 ± 20 nm and detected at 525 ± 25 nm. Regions of interest (ROIs) encompassing individual neurons were defined *a priori*. The ratio of fluorescence excited by 340 nm divided by fluorescence excited by 380 nm ($R_{340/380}$) was determined on a pixel-by-pixel basis and was averaged for each ROI. An additional background area was recorded in each field for off-line subtraction of background fluorescence. Healthy neurons were chosen based on their morphology under differential interference contrast (DIC) microscopy. In a pilot test, all selected neurons (> 100) exhibited robust Ca^{2+} influx in response to a depolarization stimulus (extracellular solution containing 50 mM KCl).

To measure menthol-induced Ca^{2+} influx, Tyrode solution containing 100 μM menthol was prepared from a 100 mM menthol (Sigma) stock solution (in 100% ethanol) before each experiment. After a 3 min baseline measurement in Tyrode, neurons were perfused with 100 μM menthol at 5 ml/min for 1 min followed by washing with Tyrode for 5 min. Peak responses were determined by calculating the absolute increase in $R_{340/380}$ above baseline (the average $R_{340/380}$ during the 3 min baseline measurement). A > 10% change from baseline was set as the threshold for a response.

Statistics

Data were reported as mean ± standard error of the mean. Origin 8.1 (Origin Lab) and Statistica (StatSoft) were used to perform statistical tests. Differences with $p < 0.05$ were considered statistically significant. The Shapiro–Wilk test was used to check data normality. Fisher's exact test, one-sample *t*-test or two-tailed Student's *t*-test were used where appropriate. The non-parametric Mann–Whitney *U* test or the Kruskal-Wallis analysis of variance (ANOVA) with Dunn's post hoc test was used where appropriate to analyze the differences in the soma size distribution.

Results

FG labels more dura afferent neurons than DiI

To compare the relative efficiency of the fluorescent retrograde tracers FG and DiI in labeling dural afferent neurons, we co-applied 2% FG and 2% DiI to the dura above a section of the SSS between bregma and lambda in adult mice for 14 days. Consistent with our previous study [4], the distribution of FG- and DiI-labeled (FG^+ and DiI^+, respectively) dural afferent neurons was similar, with the majority of the labeled neurons localized in the ophthalmic (V_1) division of TG (data not shown). Many dural afferent neurons were double labeled with FG and DiI (Figure 1). For each mouse, we randomly chose 240 non-

overlapping areas (0.15 mm^2 each) on TG sections and quantified the number of FG^+ and DiI^+ neurons. The number of FG^+ dural afferent neurons was 27 ± 5% higher than the number of DiI^+ neurons ($p < 0.05$, one-sample *t*-test; n = 2 male and 2 female mice, on average, 242 DiI^+ and 315 FG^+ neurons were counted from each mouse), indicating that FG labels dural afferent neurons more effectively than DiI under our experimental conditions.

Previous studies show that TG neurons innervate the skull and pericranial tissues [13, 14]. To minimize labeling of the pericranial afferent neurons, we removed the muscle and periosteal sheath on the skull before tracer application and confirmed that the tracers did not leak outside the polypropylene ring before tissue collection. That said, a small area of the skull within the ring (~4 mm^2) was inevitably exposed to the tracers along with the dura. In a control experiment with two mice (1 male, 1 female), we removed the muscle and periosteal sheath on the skull, attached the polypropylene ring and applied FG on the skull for two weeks. We examined 1 in every 3 TG serial sections from each mouse and did not find any FG labeled neurons, validating that our paradigm selectively labels dural afferent neurons but not pericranial afferents in mice.

FG labels dural afferent neurons that express TRPM8 channels in mice

We investigated whether FG can label dural afferent neurons expressing TRPM8 channels. In heterozygous *TRPM8*$^{EGFPf/+}$ mice, the EGFP signal corresponds well with the endogenous TRPM8 expression in DRG neurons [11]. In a control experiment, we tested the feasibility of segregating the FG and EGFP signals in two channels. We excited FG at 340 ± 10 nm and collected signals using a 515 nm long-pass filter. EGFP was excited at 470 ± 20 nm and the emission between 500-550 nm was collected. Signals from FG^+ dural afferent neurons in wild-type mice was not detectable in the EGFP channel; and the EGFP fluorescence from TG neurons in naïve *TRPM8*$^{EGFPf/+}$ mice was not detectable in the FG channel (Figure 2A). Thus, there was no bleed-through between the FG and EGFP signals under our experimental conditions.

We applied FG to the dura of *TRPM8*$^{EGFPf/+}$ mice and quantified the number of TG neurons containing FG and/or EGFP signals two weeks later. EGFP signal was present in 9.7 ± 0.4% of total TG neurons (Figure 2B), consistent with previous reports [4, 15-17]. We were able to detect EGFP-positive ($EGFP^+$) neurons in the FG^+ dural afferent population. On average, 3.8 ± 1.4% of FG^+ dural afferent neurons exhibited EGFP signal (Figure 2B), significantly lower than that in the total TG population (Figure 2B, $p < 0.05$, two-tailed *t*-test).

The mean cross-sectional area of $EGFP^+FG^+$ dural afferent neurons (240 ± 37 μm^2, n = 27 neurons pooled from 2 male and 2 female mice) was similar to that of the $EGFP^+$ TG neurons (193 ± 5 μm^2, n = 577 neurons, Figure 2C, $p = 0.8$, Kruskal-Wallis ANOVA with Dunn's post hoc test). Both were significantly smaller than the mean cross-sectional area of FG^+ dural afferents (328 ± 10 μm^2, n = 395 neurons pooled from 4 mice, Figure 2C, $p < 0.01$ $EGFP^+FG^+$ vs FG^+ and $p < 0.001$ $EGFP^+$ vs FG^+, respectively).

To fully visualize TRPM8-expressing neurons, we applied FG to the dura of two *TRPM8*$^{EGFPf/+}$ mice and stained TG sections with the anti-EGFP antibody. EGFP immunoreactivity (EGFP-ir) was not present in TG sections from wild-type mice, validating

the specificity of the antibody. In *TRPM8*$^{EGFPf/+}$ TG sections, EGFP-ir overlapped very well with the EGFP signal, in line with what was observed in DRG neurons [11]. EGFP signal was present in 98.2% neurons containing EGFP-ir (n = 1350 neurons from 1 male and 1 female mice); and 98.6% EGFP$^+$ neurons exhibited EGFP-ir (n = 1344 neurons from 1 male and 1 female mice). The fractions of FG$^+$ dural afferent neuron containing EGFP-ir were 3.3% and 3.5%, similar to the average percentage of FG$^+$ neurons with EGFP signal. We conclude that FG labels dural afferent neurons expressing TRPM8 channels but the abundance of TRPM8-expressing neurons in dural afferent population is significantly lower than that in total TG.

The projection of VGLUT3-expressing TG neurons to the mouse dura

We used the VGLUT3^{EGFP} mice to investigate whether VGLUT3-expressing PANs project to the mouse dura. In VGLUT3^{EGFP} mice, EGFP is exclusively expressed in neurons that are known to express VGLUT3 [12]. Specifically, all EGFP$^+$ skin afferents from the transgenic mice are physiologically identified as unmyelinated, low threshold mechanoreceptors (C-LTMRs) [12]. In a pilot study, we stained TG sections from VGLUT3^{EGFP} mice with the anti-EGFP antibody. The EGFP-ir overlapped very well with the EGFP signal (Figure 4). All EGFP$^+$ neurons exhibited EGFP-ir (n = 161 neurons from 1 male and 2 female mice), and 96.2 ± 3.8% neurons with EGFP-ir contained EGFP fluorescence (n = 174 neurons from 1 male and 2 female mice). Thus, use of EGFP antibody allows for easier detection of VGLUT3-expressing neurons but does not increase the abundance of this population in TG.

We applied FG to the dura of VGLUT3^{EGFP} mice and quantified the number of TG neurons containing FG and/or EGFP-ir signals two weeks later. The EGFP signal from TG neurons in naïve VGLUT3^{EGFP} mice was not detectable in the FG channel (Figure 4), indicating that EGFP signal does not interfere with the FG fluorescence. We found that 5.7 ± 1.8% of FG$^+$ dural afferent neurons were positive for EGFP-ir, which is similar to the percentage of total TG neurons containing EGFP-ir (6.7 ± 0.8%, Figure 5B). The mean cross-sectional area of EGFP$^+$FG$^+$ dural afferent neurons (218 ± 20 μm^2, n = 54 neurons pooled from 2 male and 2 female mice) was similar to that of the VGLUT3-expressing EGFP$^+$ TG neurons (228 ± 4 μm^2, n = 479 neurons pooled from 2 male and 2 female mice, Figure 5C). Both were significantly smaller than the mean cross-sectional area of FG$^+$ dural afferents (377 ± 10 μm^2, n = 511 neurons pooled from 2 male and 2 female mice, Figure 5C, $p < 0.001$, Kruskal-Wallis ANOVA with Dunn's post hoc test). We conclude that the percentage of VGLUT3-expressing neurons in dural afferents is comparable to that in the total TG population. Furthermore, VGLUT3 is exclusively expressed in small-diameter dural afferent neurons (< 500 μm^2 cross-sectional area).

A recent study reported substantial overlap between the expression of TRPM8 and VGLUT3 in unmyelinated, small-diameter DRG neurons [10], raising the possibility that TRPM8 and VGLUT3 may be co-expressed in a subpopulation of dural afferent neurons. The VGLUT3-positive cells in that study included neurons that persistently express VGLUT3 in adult mice as well as neurons that transiently express VGLUT3 during development [10]. To test whether TRPM8 is co-expressed in PANs that persistently express VGLUT3 in adult mice, we dissociated TG and lumbar DRG neurons from VGLUT3^{EGFP} mice and used the ratiometric Ca^{2+} indicator fura-2 to measure Ca^{2+} influx evoked byTRPM8 agonist menthol (100 μM,

Figure 6A). We observed menthol-induced Ca^{2+} influx in 12.4% (31/250) TG and 10.4% (14/135) DRG neurons, consistent with previous reports [16, 18-21]. However, 90% (28/31) of menthol-responsive neurons were EGFP-negative. Only 3 out of 55 (5.4%) $EGFP^+$ TG neurons responded to menthol (Figure 6B). Similarly, 4 out of 58 (6.9%) $EGFP^+$ DRG neurons were menthol-responsive. The majority (71%, 10/14) of menthol-responsive DRG neurons were EGFP-negative. As a control experiment, we measured menthol-induced Ca^{2+} influx in $EGFP^+$ TG neurons from *TRPM8*$^{EGFPf/+}$ mice. As reported [11], 90% (9/10) of $EGFP^+$ neurons responded to menthol (Figure 6B, $p < 0.001$, Fisher's exact test, compared with $EGFP^+$ neurons from $VGLUT3^{EGFP}$ mice), indicating that this dose of menthol effectively activates TRPM8 channels and EGFP signal does not interfere with fura-2 Ca^{2+} imaging under our experimental conditions. These data suggest that TRPM8 and VGLUT3 are expressed in distinct subpopulations of PANs in adult mice. It is unlikely that TRPM8 and VGLUT3 are co-expressed in dural afferent neurons.

The abundance of TG and dural afferent neurons expressing NF200

In addition to VGLUT3-expressing C-LTMRs, TG contains low- and high-threshold mechanoreceptors with myelinated Aβ or Aδ fibers. NF200 is widely used as a marker to identify these neurons [22, 23], although a small fraction of NF200-expressing ($NF200^+$) PANs has been reported to contain unmyelinated axons or exhibit c-fiber conduction velocity [24, 25]. We labeled dural afferent neurons with FG and stained the sections with an antibody against NF200 (Figure 7A). We found that 30.5 ± 2.9% of dural afferent neurons contained NF200-ir, which is similar to the percentage of $NF200^+$ neurons in total TG neuron population (38.5 ± 2.6%, Figure 7B, $p = 0.11$, two-tailed *t*-test). The mean cross-sectional area of $NF200^+FG^+$ dural afferent neurons (468 ± 24 μm^2, n = 84 neurons pooled from 1 male and 2 female mice) was similar to that of the $NF200^+$ TG neurons (469 ± 10 μm^2, n = 890 neurons pooled from 1 male and 2 female mice, $p = 0.84$, Mann–Whitney U test, Figure 7C). The majority of $NF200^+$ neurons (57%) were medium-sized neurons (> 400 μm^2 in cross-sectional area), consistent with previous studies in rats [22-24].

Discussion

In this study, we successfully labeled and quantified dural afferent neurons expressing TRPM8 channels. First, we compared the relative efficiency of FG and DiI in labeling dural afferent neurons by co-applying the same concentrations (2%) of FG and DiI onto the mouse dura for the same period of time (14 days). FG labeled more dural afferent neurons than DiI in individual mice. We speculate that the more hydrophilic FG may spread to a larger area of dura than the more lipophilic DiI, thereby accessing more dural afferent fibers. It is also possible that, compared with DiI, FG may be taken up more efficiently by dural afferent terminals and/or may require less time to be transported to the somata in TG. Secondly, we established the imaging protocol to segregate the FG and EGFP signals in TG neurons in two channels. Using FG to label dural afferent neurons in $TRPM8^{EGFPf/+}$ mice, we found that only 3-4% of dural afferent neurons express TRPM8 channels in adult mice, much lower than the percentage of total TG neurons expressing TRPM8 (10%). This is surprising, given that activation of dural TRPM8 channels significantly modifies headache-related behaviors in rodent models [6-8]. It is possible that we may underestimate the abundance of

dural afferent neurons expressing TRPM8, as we removed the muscle and periosteal sheath on the skull before tracer application. This minimizes labeling of the pericranial afferent neurons in TG, but may damage the axon collaterals of dural afferent neurons that innervate pericranial tissues through the calvarial sutures [13, 14] and cause neuronal death. Further work is needed to test whether TG neurons expressing TRPM8 project to both dura and pericranial tissues and to explore whether other methods can reveal a higher abundance of TRPM8-expressing dural afferent neurons in adult mice.

The heterogeneity of TRPM8-expressing PANs is well-documented. Some of these neurons preferentially respond to noxious cold temperatures and co-express TRPV1, TRPA1, tetrodotoxin-resistant Na^+ channels, ATP receptors as well as the receptor for artemin [26-29]. This subpopulation likely encodes cold pain and injury-induced cold allodynia. Other TRPM8-expressing PANs are activated at lower menthol concentrations or at non-noxious cooling temperature range. They likely encode cooling sensation and mediate cooling-induced analgesia. In rats, activation of dural TRPM8 channels by icilin evokes cutaneous allodynia that is blocked by sumatriptan or nitric-oxide synthase inhibitor [7]. Conversely, co-application of TRPM8 agonist menthol inhibits head-directed nocifensive behavior elicited by dural application of inflammatory mediators [6]. It is possible that both nociceptive vs non-nociceptive neurons are present within the TRPM8-expressing dural afferent population. Future experiments are necessary to retrogradely label TRPM8-expressing dural afferent neurons and to investigate the neurochemical and physiological properties of individual subpopulations.

Of note, we used $TRPM8^{EGFPf/+}$ mice maintained on CD-1 background in the present and previous studies[4, 6], not mice on C57BL6 background [11, 28]. The abundance of TRPM8-expression TG neurons, the mean soma size and the menthol-responsiveness are comparable between the two strains. That said, whether differences in genetic background can influence the abundance and/or the function of TRPM8-expressing dural afferent neurons merit further study.

A recent study reports that TRPM8 channel is mainly expressed in a subpopulation of small diameter DRG neurons that persistently express VGLUT3 in adult mice and/or transiently express VGLUT3 during development [10]. In adult mice, VGLUT3 is expressed in a discrete subpopulations of small diameter, unmyelinated PANs that does not express neuropeptide CGRP or bind to plant isolectin B4 (IB4, [12, 30, 31]). Physiological studies reveal that VGLUT3-expressing DRG neurons respond to low intensity mechanical stimulation as well as to temperature decrease below 25°C [12, 30, 31]. It is not clear whether these neurons contribute to mechanical or cold nociception [10, 12, 31, 32]. In addition to cutaneous tissues, VGLUT3-expressing PANs also project to deep tissues such as colon and bladder [33, 34], and their contribution to visceral pain also remains to be elucidated. We found that VGLUT3 is exclusively expressed in small-diameter dural afferent neurons. The percentage of VGLUT3-expressing neurons in dural afferents is comparable to that in the total TG population. In addition, the abundance of dural afferent neurons expressing NF200, a marker for Aβ and Aδ PANs with myelinated fibers, were comparable to the percentage of total TG neurons containing NF200. In rats, 80% of dural afferent C-fibers are mechanosensitive [9], some respond to low intensity stimulation. How VGLUT3-expressing dural afferents respond to

mechanical stimuli, whether they belong to C-LTMRs like their cutaneous counterparts and whether they can be sensitized by inflammatory mediators merit further study.

In the present study we measured Ca^{2+} influx evoked byTRPM8 agonist menthol in adult TG and DRG neurons from $VGLUT3^{EGFP}$ mice. This allowed us to examine TRPM8 expression in PANs that persistently express VGLUT3 in adult mice but not in those that transiently express VGLUT3 during development [10, 12, 31]. Only 5-7% $EGFP^+$ PANs responded to menthol, indicating that TRPM8 and VGLUT3 are expressed in distinct subpopulations of TG and DRG neurons in adult mice. The discrepancy between our results and the previous study results from the different mouse strains used to identify VGLUT3-expressing neurons. In the previous study, eYFP labels neurons that persistently express VGLUT3 in adult mice as well as neurons that transiently express VGLUT3 during development [10]. In this study, neurons that transiently express VGLUT3 during development are not labeled by EGFP in adult mice. It is possible that TRPM8 is expressed in PANs that transiently express VGLUT3 during development but not in PANs that persistently express VGLUT3 in adult mice. That said, all $EGFP^+$ skin afferents from thoracic DRG in $VGLUT3^{EGFP}$ mice are physiologically identified as C-LTMRs and respond to cold stimuli [12]. Whether there is higher overlap between TRPM8 and VGLUT3 expression in thoracic DRG and/or whether VGLUT3-expressing adult PANs express another cold sensor require further investigation. Taken together, we postulate that dural afferent neurons expressing TRPM8 and VGLUT3 belong to two distinct subpopulations of TG neurons. More functional studies are necessary to elucidate the contribution of TRPM8- and VGLUT3-expressing dural afferent neurons to the pathophysiology of headache.

Conclusion

TG neurons expressing TRPM8, VGLUT3 and NF200 all innervate adult mouse dura. The abundance of TRPM8-expressing neurons in dural afferent neurons is significantly lower than that in total TG neurons. The percentages of dural afferent neurons expressing VGLUT3 and NF200 are comparable to those of total TG neurons, respectively. TRPM8 and VGLUT3 are expressed in distinct subpopulations of PANs in adult mice. This provides a foundation to further investigate the role of various dural afferent subpopulations in headache pathophysiology.

Acknowledgments

We thank Drs Chang-Shen Qiu and Liang Huang for the technical help.

Financial support: This research was supported by NIH-NINDS grant R01NS083698 (YQC).

References

1. Goadsby PJ, Charbit AR, Andreou AP, Akerman S, Holland PR. Neurobiology of migraine. Neuroscience. 2009; 161:327–341. [PubMed: 19303917]
2. Pietrobon D, Moskowitz MA. Pathophysiology of migraine. Annual review of physiology. 2013; 75:365–391.
3. Strassman AM, Raymond SA, Burstein R. Sensitization of meningeal sensory neurons and the origin of headaches. Nature. 1996; 384:560–564. [PubMed: 8955268]

4. Huang D, Li SY, Dhaka A, Story GM, Cao YQ. Expression of the transient receptor potential channels TRPV1, TRPA1 and TRPM8 in mouse trigeminal primary afferent neurons innervating the dura. Molecular pain. 2012; 8:66. [PubMed: 22971321]

5. Newsom, J., Holt, JL., Neubert, JK., Caudle, R., Ahn, AH. A high density of TRPM8 expressing sensory neurons in specialized structures of the head; Society for Neuroscience Meeting Abstract; 2012.

6. Ren L, Dhaka A, Cao YQ. Function and postnatal changes of dural afferent fibers expressing TRPM8 channels. Molecular pain. 2015; 11:37. [PubMed: 26111800]

7. Burgos-Vega CC, Ahn DD, Bischoff C, et al. Meningeal transient receptor potential channel M8 activation causes cutaneous facial and hindpaw allodynia in a preclinical rodent model of headache. Cephalalgia: an international journal of headache. 2016; 36:185–193. [PubMed: 25944818]

8. Dussor G, Cao YQ. TRPM8 and Migraine. Headache. 2016; 56:1406–1417. [PubMed: 27634619]

9. Levy D, Strassman AM. Mechanical response properties of A and C primary afferent neurons innervating the rat intracranial dura. Journal of neurophysiology. 2002; 88:3021–3031. [PubMed: 12466427]

10. Draxler P, Honsek SD, Forsthuber L, Hadschieff V, Sandkuhler J. VGluT3+ Primary Afferents Play Distinct Roles in Mechanical and Cold Hypersensitivity Depending on Pain Etiology. J Neurosci. 2014; 34:12015–12028. [PubMed: 25186747]

11. Dhaka A, Earley TJ, Watson J, Patapoutian A. Visualizing cold spots: TRPM8-expressing sensory neurons and their projections. J Neurosci. 2008; 28:566–575. [PubMed: 18199758]

12. Seal RP, Wang X, Guan Y, et al. Injury-induced mechanical hypersensitivity requires C-low threshold mechanoreceptors. Nature. 2009; 462:651–655. [PubMed: 19915548]

13. Kosaras B, Jakubowski M, Kainz V, Burstein R. Sensory innervation of the calvarial bones of the mouse. The Journal of comparative neurology. 2009; 515:331–348. [PubMed: 19425099]

14. Schueler M, Messlinger K, Dux M, Neuhuber WL, De Col R. Extracranial projections of meningeal afferents and their impact on meningeal nociception and headache. Pain. 2013; 154:1622–1631. [PubMed: 23707274]

15. Abe J, Hosokawa H, Okazawa M, et al. TRPM8 protein localization in trigeminal ganglion and taste papillae. Brain research. 2005; 136:91–98. [PubMed: 15893591]

16. Bautista DM, Siemens J, Glazer JM, et al. The menthol receptor TRPM8 is the principal detector of environmental cold. Nature. 2007; 448:204–208. [PubMed: 17538622]

17. Kobayashi K, Fukuoka T, Obata K, et al. Distinct expression of TRPM8, TRPA1, and TRPV1 mRNAs in rat primary afferent neurons with adelta/c-fibers and colocalization with trk receptors. The Journal of comparative neurology. 2005; 493:596–606. [PubMed: 16304633]

18. Colburn RW, Lubin ML, Stone DJ Jr, et al. Attenuated cold sensitivity in TRPM8 null mice. Neuron. 2007; 54:379–386. [PubMed: 17481392]

19. Dhaka A, Murray AN, Mathur J, Earley TJ, Petrus MJ, Patapoutian A. TRPM8 is required for cold sensation in mice. Neuron. 2007; 54:371–378. [PubMed: 17481391]

20. McKemy DD, Neuhausser WM, Julius D. Identification of a cold receptor reveals a general role for TRP channels in thermosensation. Nature. 2002; 416:52–58. [PubMed: 11882888]

21. Peier AM, Moqrich A, Hergarden AC, et al. A TRP channel that senses cold stimuli and menthol. Cell. 2002; 108:705–715. [PubMed: 11893340]

22. Goldstein ME, House SB, Gainer H. NF-L and peripherin immunoreactivities define distinct classes of rat sensory ganglion cells. Journal of neuroscience research. 1991; 30:92–104. [PubMed: 1795410]

23. Perry MJ, Lawson SN, Robertson J. Neurofilament immunoreactivity in populations of rat primary afferent neurons: a quantitative study of phosphorylated and non-phosphorylated subunits. Journal of neurocytology. 1991; 20:746–758. [PubMed: 1960537]

24. Bae JY, Kim JH, Cho YS, Mah W, Bae YC. Quantitative analysis of afferents expressing substance P, calcitonin gene-related peptide, isolectin B4, neurofilament 200, and Peripherin in the sensory root of the rat trigeminal ganglion. The Journal of comparative neurology. 2015; 523:126–138. [PubMed: 25185935]

25. Ruscheweyh R, Forsthuber L, Schoffnegger D, Sandkuhler J. Modification of classical neurochemical markers in identified primary afferent neurons with Abeta-, Adelta-, and C-fibers

after chronic constriction injury in mice. The Journal of comparative neurology. 2007; 502:325–336. [PubMed: 17348016]

26. Lippoldt EK, Elmes RR, McCoy DD, Knowlton WM, McKemy DD. Artemin, a glial cell line-derived neurotrophic factor family member, induces TRPM8-dependent cold pain. J Neurosci. 2013; 33:12543–12552. [PubMed: 23884957]
27. Sarria I, Ling J, Xu GY, Gu JG. Sensory discrimination between innocuous and noxious cold by TRPM8-expressing DRG neurons of rats. Molecular pain. 2012; 8:79. [PubMed: 23092296]
28. Takashima Y, Ma L, McKemy DD. The development of peripheral cold neural circuits based on TRPM8 expression. Neuroscience. 2010; 169:828–842. [PubMed: 20580783]
29. Teichert RW, Raghuraman S, Memon T, et al. Characterization of two neuronal subclasses through constellation pharmacology. Proceedings of the National Academy of Sciences of the United States of America. 2012; 109:12758–12763. [PubMed: 22778416]
30. Li L, Rutlin M, Abraira VE, et al. The functional organization of cutaneous low-threshold mechanosensory neurons. Cell. 2011; 147:1615–1627. [PubMed: 22196735]
31. Lou S, Duan B, Vong L, Lowell BB, Ma Q. Runx1 controls terminal morphology and mechanosensitivity of VGLUT3-expressing C-mechanoreceptors. J Neurosci. 2013; 33:870–882. [PubMed: 23325226]
32. Peirs C, Williams SP, Zhao X, et al. Dorsal Horn Circuits for Persistent Mechanical Pain. Neuron. 2015; 87:797–812. [PubMed: 26291162]
33. Brumovsky PR. VGLUTs in Peripheral Neurons and the Spinal Cord: Time for a Review. ISRN neurology. 2013; 2013:829753. [PubMed: 24349795]
34. Brumovsky PR, Seal RP, Lundgren KH, Seroogy KB, Watanabe M, Gebhart GF. Expression of vesicular glutamate transporters in sensory and autonomic neurons innervating the mouse bladder. The Journal of urology. 2013; 189:2342–2349. [PubMed: 23159277]

Abbreviations

PAN	primary afferent neuron
CGRP	calcitonin gene-related peptide
TRPM8	transient receptor potential melastatin 8
TG	trigeminal ganglion
DiI	1,1′-dioctadecyl-3,3,3′,3′-tetramethylindocarbocyanine perchlorate
FG	Fluoro-Gold
C-LTMR	unmyelinated low threshold mechanoreceptor
VGLUT3	vesicular glutamate transporter 3
DRG	dorsal root ganglion
NF200	neurofilament 200
-ir	-immunoreactivity
EGFP	enhanced green fluorescent protein
SSS	superior sagittal sinus
ROI	region of interest

ANOVA analysis of variance

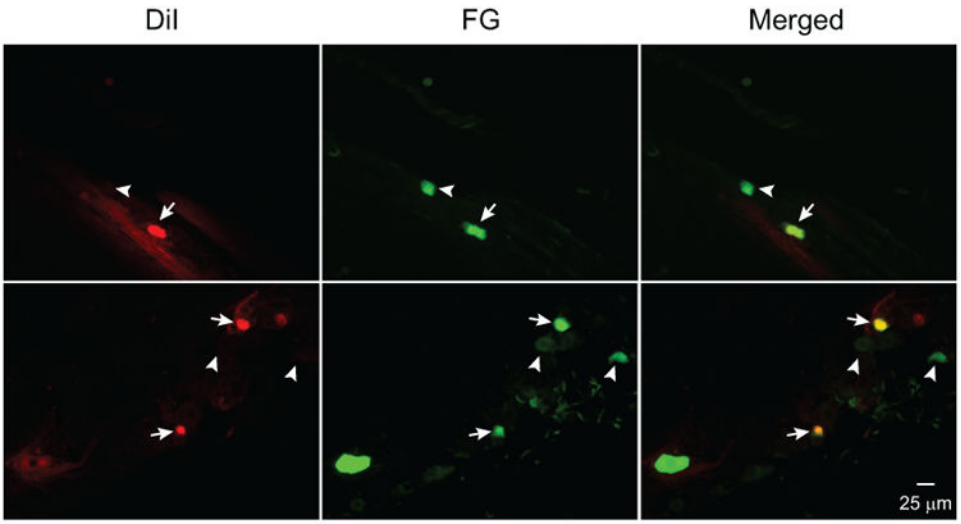

Figure 1. FG labels more dura afferent neurons than DiI

Representative images of two TG sections showing DiI- and FG-labeled dural afferent neurons. The arrows indicate double-labeled neurons. The thick and thin arrowheads indicate neurons with only FG and DiI labeling, respectively.

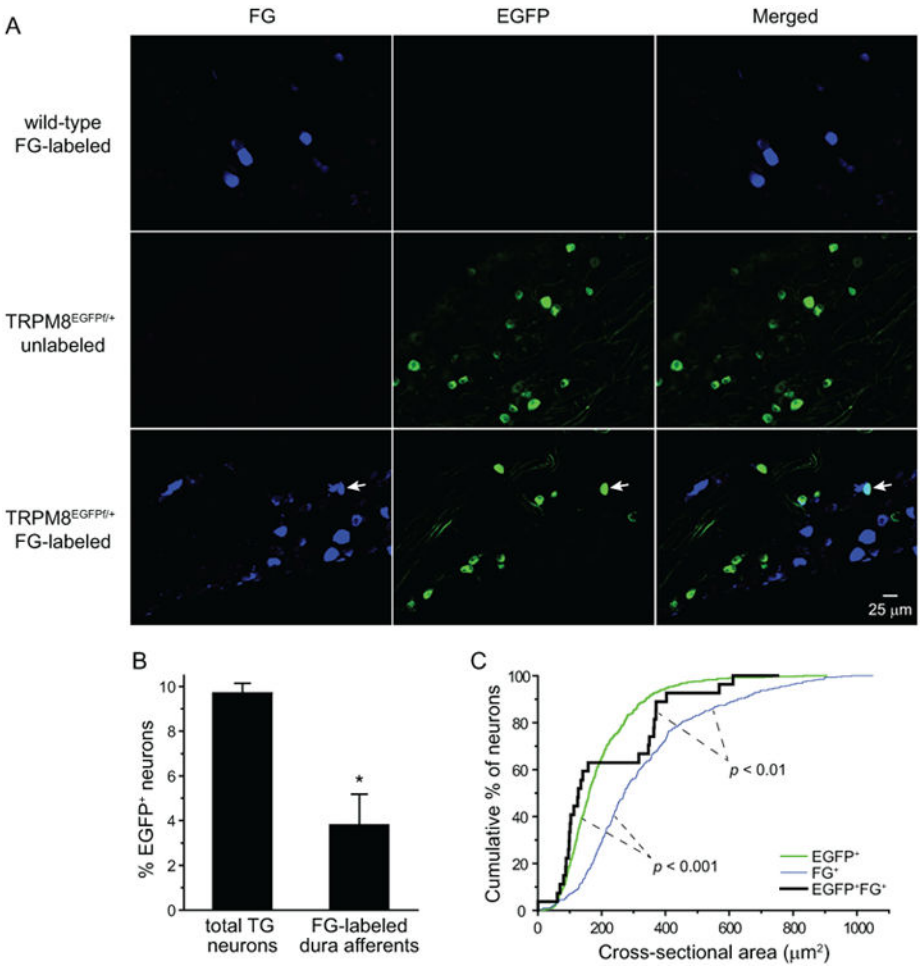

Figure 2. The distribution of neurons expressing TRPM8 channels in TG and dural afferent neurons

(A) Representative images of TG sections from a wild-type mouse with dural FG application and TRPM8$^{EGFPf/+}$ mice with and without dural FG labeling, respectively. The arrows indicate a FG$^+$ dural afferent neuron that is also EGFP$^+$.

(B) The percentages of EGFP$^+$ neurons in total TG population and in FG$^+$ dural afferent neurons in TRPM8$^{EGFPf/+}$ mice receiving dural FG application (n = 2 male and 2 female mice; on average, 2380 TG neurons and 100 FG$^+$ neurons were counted from each mouse; *$p < 0.05$, two-tailed *t*-test).

(C) Cumulative distributions of the cross-sectional areas of EGFP$^+$, FG$^+$ and EGFP$^+$FG$^+$ neurons (n = 577, 395 and 27 neurons pooled from 4 mice, respectively; same neurons as in **B**). The sizes of EGFP$^+$ and EGFP$^+$FG$^+$ neurons are significantly smaller than that of the FG$^+$ dural afferent neurons ($p < 0.001$ and $p < 0.01$, respectively, Kruskal-Wallis ANOVA with Dunn's post hoc test). The sizes of EGFP$^+$ and EGFP$^+$FG$^+$ neurons are comparable ($p = 0.8$).

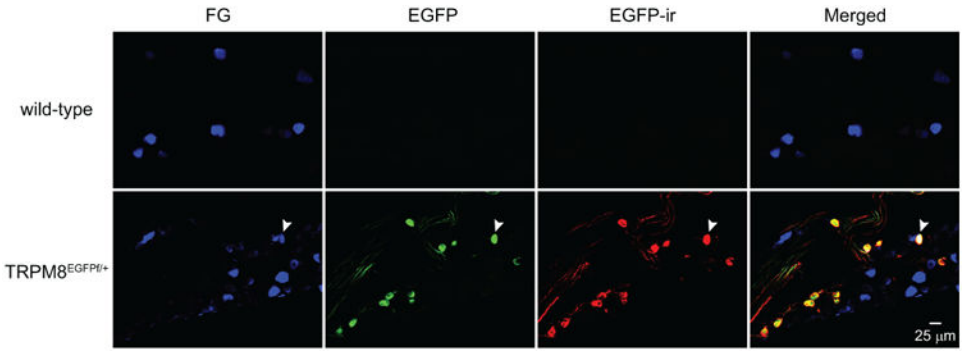

Figure 3. Overlap between EGFP signal and EGFP-ir in TG and dural afferent neurons from *TRPM8*$^{EGFPf/+}$ mice

Representative images of TG sections from wild-type and TRPM8$^{EGFPf/+}$ mice with dural FG application, respectively. The EGFP signal and EGFP-ir overlap well in the TRPM8$^{EGFPf/+}$ section. Neither is present in the wild-type section, validating the specificity of the EGFP antibody. The arrows indicate a FG^{+} dural afferent neuron that exhibits both EGFP signal and EGFP-ir.

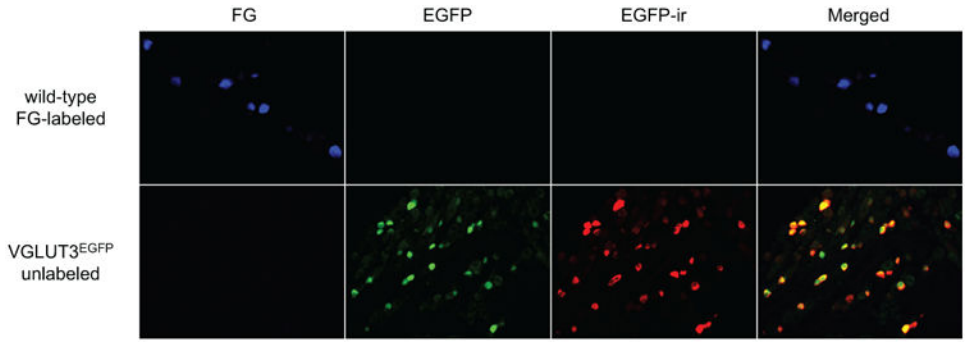

Figure 4. VGLUT3-expressing TG neurons detected by EGFP signal and EGFP-ir

Representative images of TG sections from a wild-type mouse with dural FG application and a VGLUT3^{EGFP} mouse without dural FG labeling, respectively. The EGFP signal and EGFP-ir overlap well in the VGLUT3^{EGFP} section. Neither is present in the wild-type TG section. EGFP signal does not bleed into the FG channel; and FG fluorescence does not interfere with the EGFP or EGFP-ir signals.

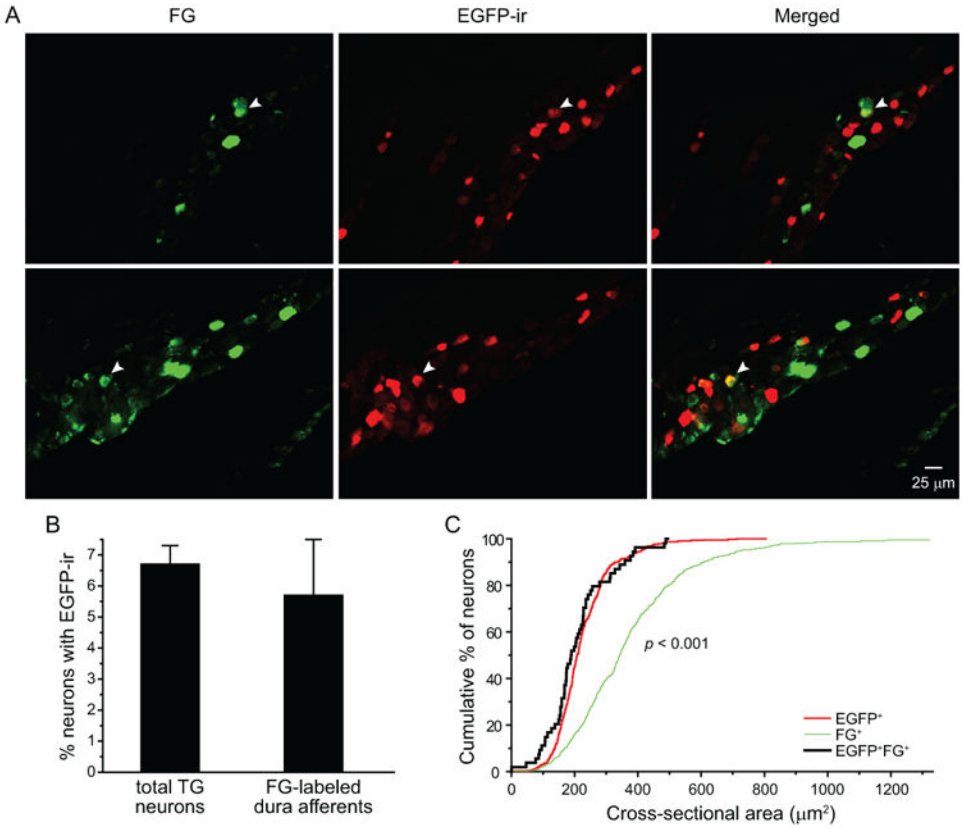

Figure 5. The distribution of VGLUT3-expressing neurons in TG and dural afferent neurons

(A) Representative images of two TG sections from VGLUT3^{EGFP} mice with dural application of FG. The arrowheads indicate FG$^+$ dural afferent neurons that are also EGFP$^+$.

(B) The percentages of TG neurons and FG$^+$ dural afferent neurons that are EGFP$^+$ (n = 2 male and 2 femalemice; on average, 1360 TG neurons and 127 FG$^+$ neurons were counted from each mouse; p = 0.44, two-tailed *t*-test).

(C) Cumulative distributions of the cross-sectional areas of EGFP$^+$, FG$^+$ and EGFP$^+$FG$^+$ neurons (n = 479, 511 and 54 neurons pooled from 4 mice, respectively; same neurons as in **B**). The sizes of EGFP$^+$ and EGFP$^+$FG$^+$ neurons are significantly smaller than that of the FG$^+$ dural afferent neurons ($p < 0.001$, Kruskal-Wallis ANOVA with Dunn's post hoc test).

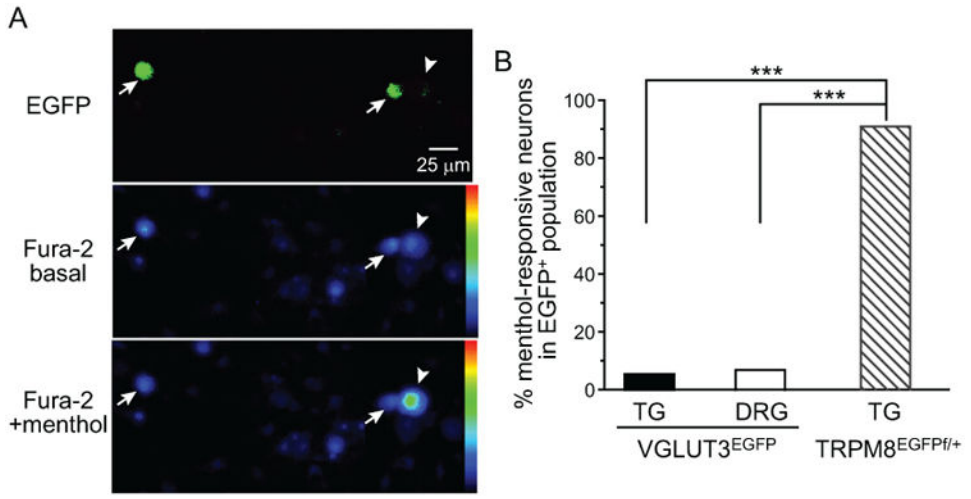

Figure 6. The response to TRPM8 agonist menthol in TG neurons from VGLUT3^{EGFP} mice

(A) Representative images of dissociated TG neurons from VGLUT3^{EGFP} mice. Upper panel: EGFP signal. Middle and lower panels: representative Fura-2 images before and after application of 100 μM menthol, respectively. The blue to green color transition reflects increase in intracellular Ca^{2+}. The arrows and arrowheads indicate EGFP^{+} and EGFP-negative (EGFP^{-}) neurons, respectively.

(B) The percentages of menthol-responsive neurons in 55 EGFP^{+} TG neurons and 58 EGFP^{+} DRG neurons cultured from 10 VGLUT3^{EGFP} mice (5 male and 5 female). An additional 10 EGFP^{+} neurons were cultured from 3 (2 male, 1 female) TRPM8$^{EGFPf/+}$ mice (***$p < 0.001$, Fisher's exact test).

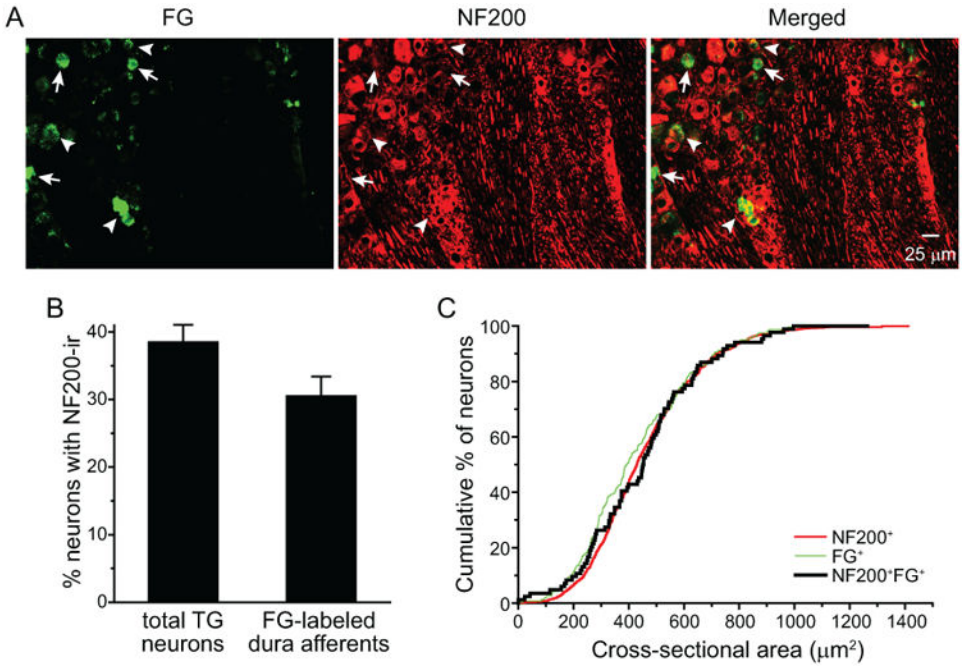

Figure 7. The distribution of NF200$^+$ neurons in total TG and dural afferent populations

(A) Representative images of a TG section containing FG$^+$ dural afferent neurons and NF200-labeled neurons. Arrowheads indicate neurons that are both FG$^+$ and NF200$^+$.

(B) The percentages of TG neurons and FG$^+$ dural afferent neurons that are NF200$^+$ (n = 1 male and 2 female mice; on average, 1700 TG neurons and 120 FG$^+$ neurons were counted from each mouse; p = 0.11, two-tailed *t*-test).

(C) Cumulative distributions of the cross-sectional areas of NF200$^+$, FG$^+$ and NF200$^+$FG$^+$ neurons (n = 890, 240 and 84 neurons pooled from 3 mice, respectively; same neurons as in **B**). The sizes distributions of NF200$^+$, FG$^+$ and NF200$^+$FG$^+$ neurons are similar (p = 0.11, Kruskal-Wallis ANOVA).